

Molecular understanding of atmospheric particle formation from sulfuric acid and large oxidized organic molecules

Siegfried Schobesberger^{a,1}, Heikki Junninen^a, Federico Bianchi^b, Gustaf Lönn^a, Mikael Ehn^a, Katrianne Lehtipalo^a, Josef Dommen^b, Sebastian Ehrhart^c, Ismael K. Ortega^a, Alessandro Franchin^a, Tuomo Nieminen^{a,d}, Francesco Riccobono^b, Manuel Hutterli^e, Jonathan Duplissy^{a,d}, João Almeida^c, Antonio Amorim^f, Martin Breitenlechner^g, Andrew J. Downard^h, Eimear M. Dunne^{ij}, Richard C. Flagan^h, Maija Kajos^a, Helmi Keskinen^k, Jasper Kirkby^l, Agnieszka Kupc^m, Andreas Kürten^c, Theo Kurténⁿ, Ari Laaksonen^{k,o}, Serge Mathot^l, Antti Onnela^l, Arnaud P. Praplan^{b,2}, Linda Rondo^c, Filipe D. Santos^f, Simon Schallhart^a, Ralf Schnitzhofer^g, Mikko Sipilä^a, António Tomé^f, Georgios Tsagkogeorgas^p, Hanna Vehkamäki^a, Daniela Wimmer^{a,c}, Urs Baltensperger^b, Kenneth S. Carslawⁱ, Joachim Curtius^c, Armin Hansel^{g,q}, Tuukka Petäjä^a, Markku Kulmala^a, Neil M. Donahue^r, and Douglas R. Worsnop^{a,i,p,s}

^aDepartment of Physics, University of Helsinki, 00014 Helsinki, Finland; ^bLaboratory of Atmospheric Chemistry, Paul Scherrer Institute, 5232 Villigen PSI, Switzerland; ^cInstitute for Atmospheric and Environmental Sciences, Goethe University Frankfurt, 60438 Frankfurt am Main, Germany; ^dHelsinki Institute of Physics, University of Helsinki, 00014 Helsinki, Finland; ^eTofwerk AG, 3600 Thun, Switzerland; ^fLaboratory for Systems, Instrumentation and Modeling in Science and Technology for Space and the Environment, University of Lisbon and University of Beira Interior, 1749-016 Lisbon, Portugal; ^gInstitute for Ion and Applied Physics, University of Innsbruck, 6020 Innsbruck, Austria; ^hDivision of Chemistry and Chemical Engineering, California Institute of Technology, Pasadena, CA 91125; ⁱSchool of Earth and Environment, University of Leeds, Leeds LS2 9JT, United Kingdom; ^jFinnish Meteorological Institute, Kuopio Unit, 70211 Kuopio, Finland; ^kDepartment of Applied Physics, University of Eastern Finland, 70211 Kuopio, Finland; ^lEuropean Organization for Nuclear Research, 1211 Geneva, Switzerland; ^mFaculty of Physics, University of Vienna, 1090 Vienna, Austria; ⁿDepartment of Chemistry, University of Helsinki, 00014 Helsinki, Finland; ^oFinnish Meteorological Institute, 00101 Helsinki, Finland; ^pPhysics Department, Leibniz Institute for Tropospheric Research, 04318 Leipzig, Germany; ^qIonicon Analytik GmbH, 6020 Innsbruck, Austria; ^rCenter for Atmospheric Particle Studies, Carnegie Mellon University, Pittsburgh, PA 15213; ^sAerodyne Research, Billerica, MA 01821

Edited by Mark H. Thiemens, University of California, San Diego, La Jolla, CA, and approved September 5, 2013 (received for review April 12, 2013)

Atmospheric aerosols formed by nucleation of vapors affect radiative forcing and therefore climate. However, the underlying mechanisms of nucleation remain unclear, particularly the involvement of organic compounds. Here, we present high-resolution mass spectra of ion clusters observed during new particle formation experiments performed at the Cosmics Leaving Outdoor Droplets chamber at the European Organization for Nuclear Research. The experiments involved sulfuric acid vapor and different stabilizing species, including ammonia and dimethylamine, as well as oxidation products of pinanediol, a surrogate for organic vapors formed from monoterpenes. A striking resemblance is revealed between the mass spectra from the chamber experiments with oxidized organics and ambient data obtained during new particle formation events at the Hyytiälä boreal forest research station. We observe that large oxidized organic compounds, arising from the oxidation of monoterpenes, cluster directly with single sulfuric acid molecules and then form growing clusters of one to three sulfuric acid molecules plus one to four oxidized organics. Most of these organic compounds retain 10 carbon atoms, and some of them are remarkably highly oxidized (oxygen-to-carbon ratios up to 1.2). The average degree of oxygenation of the organic compounds decreases while the clusters are growing. Our measurements therefore connect oxidized organics directly, and in detail, with the very first steps of new particle formation and their growth between 1 and 2 nm in a controlled environment. Thus, they confirm that oxidized organics are involved in both the formation and growth of particles under ambient conditions.

aerosol particles | atmospheric nucleation | atmospheric chemistry | mass spectrometry

Atmospheric new particle formation (often referred to as nucleation) plays an important yet uncertain role in climate. Particles with diameter (D_p) larger than about 50 nm can serve as seeds for the condensation of water to form cloud droplets [cloud condensation nuclei (CCN)]. Cloud properties such as albedo and lifetime are in turn sensitive to CCN number concentrations.

Changes to CCN number concentrations from preindustrial times constitute a major uncertainty in estimates of anthropogenic climate forcing (1). New particle formation dominates the total number concentrations of atmospheric aerosol particles; however, newly formed particles must grow from $D_p \sim 1.5$ to $D_p \sim 50\text{--}100$ nm to be able to act as CCN, and the vast majority are

Significance

The formation of nanoparticles by condensable vapors in the atmosphere influences radiative forcing and therefore climate. We explored the detailed mechanism of particle formation, in particular the role of oxidized organic molecules that arise from the oxidation of monoterpenes, a class of volatile organic compounds emitted from plants. We mimicked atmospheric conditions in a well-controlled laboratory setup and found that these oxidized organics form initial clusters directly with single sulfuric acid molecules. The clusters then grow by the further addition of both sulfuric acid and organic molecules. Some of the organics are remarkably highly oxidized, a critical feature that enables them to participate in forming initial stable molecular clusters and to facilitate the first steps of atmospheric nanoparticle formation.

Author contributions: S. Schobesberger, K.L., A.F., J. Duplissy, R.C.F., J.K., A.L., S.M., A.O., F.D.S., M.S., U.B., K.S.C., J.C., A.H., T.P., M. Kulmala, N.M.D., and D.R.W. designed research; S. Schobesberger, F.B., K.L., S.E., I.K.O., A.F., T.N., F.R., J. Duplissy, J.A., M.B., A.J.D., E.M.D., M. Kajos, H.K., J.K., A. Kupc, A. Kürten, T.K., A.P.P., L.R., S. Schallhart, R.S., G.T., and D.W. performed research; H.J., G.L., M.E., K.L., M.H., T.K., H.V., and D.R.W. contributed new reagents/analytic tools; S. Schobesberger, H.J., F.B., M.E., K.L., J. Dommen, S.E., I.K.O., A.F., T.N., F.R., J.A., A.A., M.B., A.P.P., L.R., R.S., and A.T. analyzed data; and S. Schobesberger and N.M.D. wrote the paper.

The authors declare no conflict of interest.

This article is a PNAS Direct Submission.

¹To whom correspondence should be addressed. E-mail: siegfried.schobesberger@helsinki.fi.

²Present address: Department of Physics, University of Helsinki, 00014 Helsinki, Finland.

This article contains supporting information online at www.pnas.org/lookup/suppl/doi:10.1073/pnas.1306973110/-DCSupplemental.

lost due to coagulation (2). Formation and growth of particles are separate but coupled problems, likely involving contributions from different species (3, 4). It is imperative that we understand both these problems to understand and predict past and future changes to the CCN budget as both climate and emissions change in the future.

There is strong evidence that atmospheric new particle formation nearly always involves clusters with at least one molecule of sulfuric acid (5–8). However, sulfuric acid is not abundant enough in the atmosphere to alone explain the observed formation rates of new particles (9). It remains unclear how other compounds participate, but clusters involving sulfuric acid may be stabilized by electric charge, water vapor, bases such as ammonia and amines (9–12), and oxidized organics (13–16). The formation of stable clusters is a distinct critical step in atmospheric new particle formation (3). The stabilizing agents probably compete for importance in different parts of the atmosphere, depending on their availability (17).

Previous research suggests that oxidized organics may take part in both particle formation and in subsequent particle growth from $D_p \sim 1.5$ to $D_p \sim 10$ nm (15, 18, 19). Their role, however, remains controversial. Specifically, it is argued that the high saturation vapor pressure of organics renders them incapable of condensing onto particles smaller than 3 or 4 nm (20, 21), whereas other studies suggest that they are, in fact, capable of doing so (22). Experiments that show clear evidence that organic acids can combine with sulfuric acid to form initial clusters have been conducted at concentrations several orders of magnitude higher than those typically found in the atmosphere. None has directly measured the composition of the clusters and nanoparticles as they form. There is strong evidence that condensation of something other than sulfuric acid contributes to accelerating particle growth from 1.5 nm onward. The most likely candidate is organic vapors (3, 23–25). Thus far, however, measurements have failed to resolve exactly how organics participate in new particle formation or at which particle size their involvement begins (4).

Current research aims at isolating and determining the critical processes involved in the formation of molecular clusters and their subsequent growth into particles. Experimental isolation of these critical processes is challenging, because they involve extremely low concentrations of participating vapors: sulfuric acid vapor concentrations $[H_2SO_4]$ are typically in the range of 10^6 to 10^7 cm^{-3} , and, with the exception of water, the stabilizers may be only slightly more abundant. Few particle formation experiments have directly measured particle numbers and growth rates in the critical 1- to 2-nm size range. Even fewer have effectively constrained the chemistry (composition) of clusters over that range.

For this study, we used techniques that have emerged only over the last few years to constrain the composition of nucleating clusters under ambient conditions (26). The objective was to establish key composition signatures of the clusters over the critical 1- to 2-nm size range. These chemical fingerprints of new particle formation events can then be compared with ambient observations. The objective was achieved via carefully controlled particle formation experiments at the Cosmics Leaving Outdoor Droplets (CLOUD) aerosol chamber at the European Organization for Nuclear Research (CERN), in Switzerland, during the CLOUD 4 campaign (*SI Text*). The CLOUD chamber enables precise control of experimental parameters and provides the exceptionally clean experimental conditions that are essential when performing experiments with extremely low concentrations of participating vapors.

The oxidation of monoterpenes is an important source of condensable species (27) that may contribute to the formation and early growth of atmospheric particles (22, 28). The present study focuses on one branch of the oxidation chemistry of α -pinene as a model for the broad class of monoterpenes that are important in the atmosphere. We used pinanediol (PD, $C_{10}H_{18}O_2$) as a

surrogate first-generation oxidation product of monoterpenes. It has the advantage of not being attacked by ozone due to its lack of double bonds, making its oxidation controllable by varying UV illumination. We also use data from earlier CLOUD campaigns, examining the role of ammonia (9) and dimethylamine (DMA) (29), as we develop an extensive set of chemical fingerprints for the process of new particle formation.

Results and Discussion

A unique aspect of the CLOUD measurements is that they are, to the best of our knowledge, the first to independently vary and measure cluster compositions and vapor concentrations over ranges found in the atmosphere. The focus of this work is to identify the molecules that form new particles to understand the mechanism underlying particle formation and initial growth. Central to this paper is the high-resolution atmospheric pressure interface time-of-flight (API-TOF; Tofwerk AG and Aerodyne Research) mass spectrometer (26), which allows us to constrain the chemical composition of newly formed and growing molecular ion clusters (see *SI Text* for more details). Mass spectra are plotted as mass defect plots, with the exact mass of a compound on the abscissa and the deviation from the nominal (integer) mass (i.e., the mass defect) on the ordinate (Fig. 1). Peaks are plotted as circles with areas scaled by ion count rates. These plots are especially useful for the diagnosis of growth involving specific molecules and for diagnosing progressive oxidation of organic species; each generates characteristic patterns in the mass defect space, as we shall describe.

The API-TOF spectra reveal the abundance and chemical composition of negatively and positively charged ions and ionic clusters within the CLOUD chamber. Small molecular clusters in the CLOUD chamber have a lifetime of about 8 min against their major loss process of collision with the chamber walls. Therefore there is sufficient time for the charge distribution to approach steady state (30). We will argue that the composition of the negatively charged clusters, described here, and that of the neutral clusters are similar.

New Particle Formation in the CLOUD Chamber in Comparison with Ambient Observations. Earlier experiments in CLOUD focused on H_2SO_4 + ammonia and H_2SO_4 + DMA systems (Fig. 1 *A* and *B*) (9, 29). The formation and initial growth of clusters was found to proceed by acid-base interactions. Both systems show a remarkably similar behavior in the API-TOF data; the clusters grow with a H_2SO_4 :base stoichiometry very close to 1:1, becoming slightly less acidic as they grow (full neutralization of sulfuric acid with regard to its acidity occurs at a stoichiometry of 1:2). In these negative ions, the HSO_4^- ion serves as a Lewis base, acting as proton acceptor like the regular bases ammonia and DMA. The preferred composition thus involves a higher sulfur-to-nitrogen ratio for the negatively charged case than expected for the electrically neutral case; e.g., mostly $n:(n-1)$ for the initial anion clusters in H_2SO_4 + DMA systems and about $n:(n-3)$ in H_2SO_4 + ammonia systems. The concentrations of base vapors for these experiments were nearly always at least 10 times the acid vapor concentration. Thus, in these systems, cluster growth was rate limited by the arrival of H_2SO_4 molecules.

Data from later experiments (Fig. 1 *C*) are strikingly different: the spectra following SO_2 and PD oxidation form broad bands oriented diagonally from the upper left to lower right, ~ 220 Thomson (Th) apart from each other. Each band consists (as described below) largely of molecular clusters containing oxidized $C_{10}H_xO_y$ organics (one in the first band, two in the second band, etc.), an HSO_4^- ion, and zero to three additional H_2SO_4 molecules. Although the succession of bands indicates progressive addition of $C_{10}H_xO_y$ molecules, the number of H_2SO_4 molecules in the clusters increases as well, suggesting that

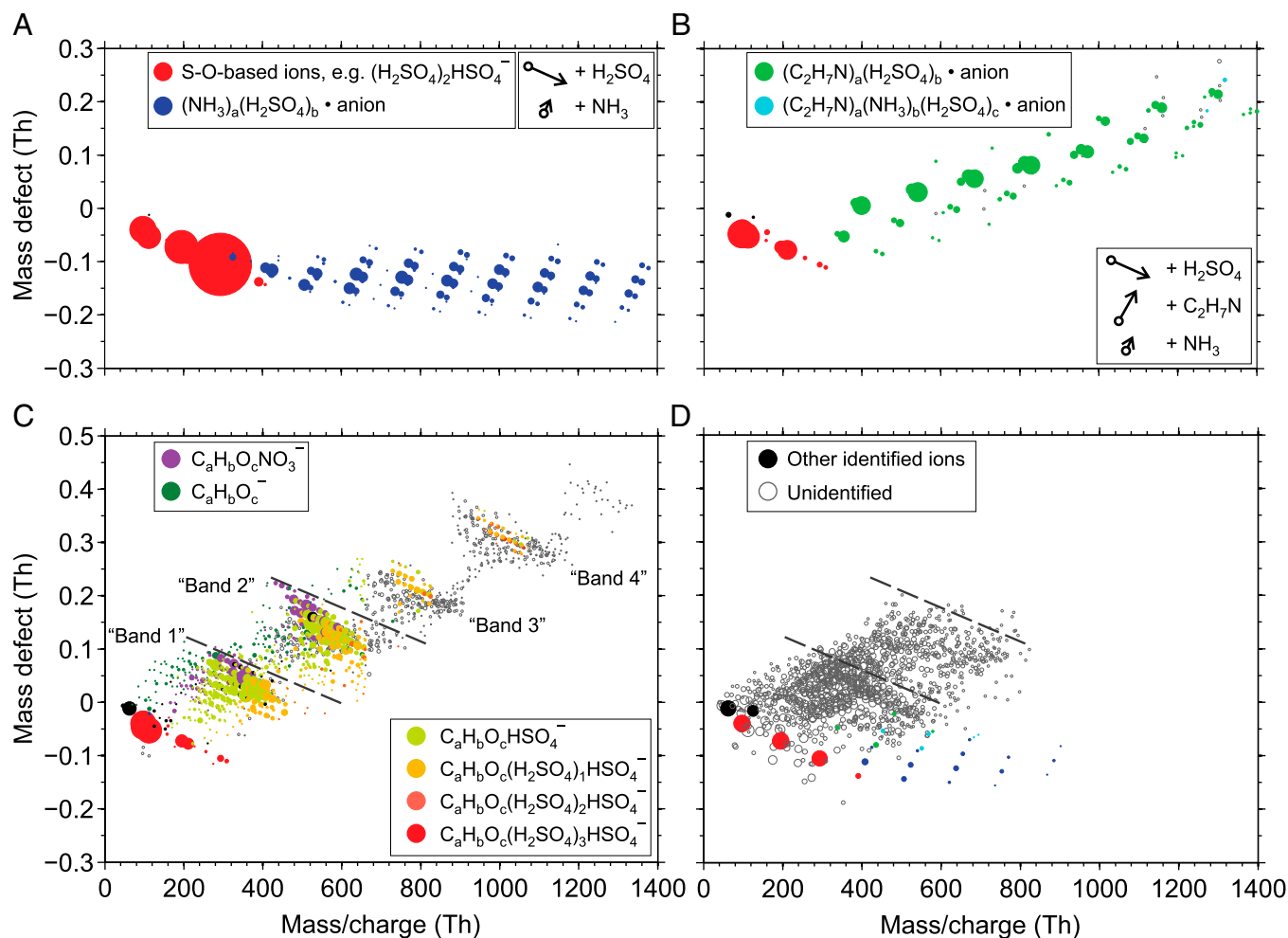


Fig. 1. API-TOF mass defect diagrams for negatively charged clusters during new particle formation experiments at the CLOUD chamber (A–C) and in a boreal forest environment (D). B is adapted from Almeida et al. (29). The ion mass is shown on the x axis (units Th = Da/e); the mass defect (the difference between the exact mass and the nominal mass) is shown on the y axis. Circle diameters are proportional to (count rates)^{1/2} (A–C, for proportionality of the circle areas) or to log₁₀(count rates)² (D, for better visibility of weaker signals). Colors indicate the composition of certain identified ions; the legends are shared between all panels. Other identified ions are shown in black. Unidentified ions are shown as open gray circles. Experiments at the CLOUD chamber show new particle formation and growth for systems including H₂SO₄ and ammonia (NH₃) (A), H₂SO₄ and DMA (C₂H₇N) (B), and gas-phase oxidation products of PD (C), a surrogate for first-generation oxidation products of monoterpenes. Observations during new particle formation in the boreal forest at Hyttiälä, Finland (D), show both clusters of small bases and sulfuric acid, as well as features broadly consistent with the PD oxidation experiment. Dashed lines are added as reference (C and D).

coaddition of organics and H₂SO₄ occurs without favoring a specific stoichiometry.

The CLOUD data in Fig. 1A–C may be compared with spectra observed during new particle formation events at the boreal forest research station in Hyttiälä, Finland (Fig. 1D). This spectrum shows features from all of the investigated systems, as H₂SO₄-base clusters are present involving both ammonia and DMA, although mainly ammonia. However, the vast majority of the ion signal lies within two bands that resemble the bands in Fig. 1C, again containing a variety of oxidized organics (28). The organics have a broader range of carbon numbers than in the CLOUD data, although C₁₀ is still abundant, as expected in an environment where oxidation products of monoterpenes dominate the oxidized organics. Within the first band, several individual C₁₀ molecular formulae observed in CLOUD appear also in the ambient spectrum. The location of the corresponding peaks in the mass defect plot confirms that many of these organics are highly oxidized (see *SI Text* for details).

Particle formation rates provide an additional constraint on the formation mechanism when comparing laboratory and field

data (indeed, until now the only constraint). The formation rates for 1.7-nm particles ($J_{1.7}$) for both the H₂SO₄ + DMA (29) and H₂SO₄ + organics experiments compare favorably with field data, with $J_{1.7} \leq 100 \text{ cm}^{-3} \cdot \text{s}^{-1}$ and $J_{1.7} \sim 10 \text{ cm}^{-3} \cdot \text{s}^{-1}$, respectively, at $[\text{H}_2\text{SO}_4] = 10^7 \text{ cm}^{-3}$. However, the H₂SO₄ + ammonia experiments (9) resulted in particle formation rates at least an order of magnitude smaller than those observed in the field under comparable conditions (7, 18, 31). Consequently, the combination of particle formation rates and cluster chemistry (Fig. 1) suggests that oxidized organics are involved in the formation of new particles in the observed boreal forest events, together with H₂SO₄. Bonds between H₂SO₄ and bases likely play a supporting role.

Role of Oxidized Organic Compounds in the Chemical Composition of Ion Clusters. Elemental compositions could be clearly assigned to most ions up to the end of band 2 in Fig. 1C. Fig. 2A zooms in on band 1, revealing that many of the peaks fall on a regular grid corresponding to ions with the general formula $\text{HSO}_4^- \cdot \text{C}_{10}\text{H}_x\text{O}_y$, where x (n_H) = 12, 14, 16 and y (n_O) = 2–12. Signals from these

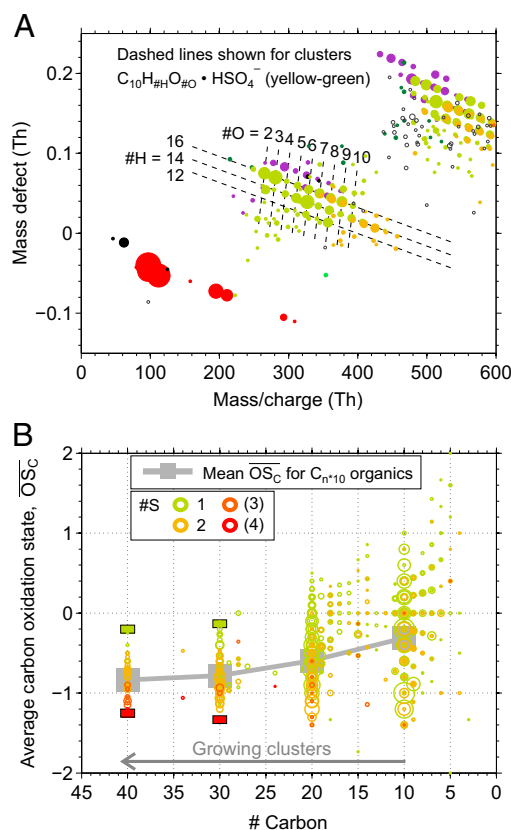


Fig. 2. (A) Mass defect diagram for a part of an anion mass spectrum during a new particle formation event. The composition of oxidized organic compounds can be identified by the exact ion mass, translating to a certain position in this diagram, as visualized by dashed lines for clusters $C_{10}H_xO_y \bullet HSO_4^-$. Color coding follows Fig. 1. (B) $\overline{OS}_C = 2 \frac{\#O}{\#C} - \frac{\#H}{\#C}$ for oxidized organics ($C_xH_yO_z$) within clusters of the type $C_xH_yO_z \bullet (H_2SO_4)_m \bullet HSO_4^-$ ($m = 0, 1, \dots$), shown against their carbon atom content. Circle areas are proportional to ion counts; colors denote different numbers of H_2SO_4 involved. Rectangles at $\#C = 30$ and $\#C = 40$ represent lower and upper limits for the \overline{OS}_C of identified ions assuming one H_2SO_4 has been misidentified with H_2O_6 and vice versa. Large gray squares in the background mark the mean \overline{OS}_C for C_{n+10} organics, connected by gray lines to guide the eye.

compounds are shown with yellow-green circles. There is a second group of peaks embedded in the band but offset by the coordinates of H_2SO_4 ($\Delta x = 97.967$ Th, $\Delta y = -0.033$ Th), corresponding to similar clusters containing an additional H_2SO_4 . This group is shown with orange-colored circles. Along the top of the band is a group of similar organics clustered with contaminant nitrate (NO_3^-) instead of bisulfate (HSO_4^-). These nitrate peaks, shown in purple, reveal strong clustering between NO_3^- and the oxidized organics. These peaks dominated the anion spectrum at conditions of low concentrations of H_2SO_4 ($< 5.8 \times 10^5$ cm^{-3}). However, they showed no relation to particle formation in our experiments. The nitrate peaks will thus be excluded from the following analysis. Similar clusters formed by organic compounds and NO_3^- or HSO_4^- have also been observed in the boreal forest (28).

We characterize the products of PD oxidation via the average oxidation state of carbon $\overline{OS}_C = 2 n_O : n_C - n_H : n_C$ (32), where n_O , n_C , and n_H are the numbers of oxygen, carbon, and hydrogen atoms attributed to the organic part of an identified ion cluster, respectively. Fig. 2B shows \overline{OS}_C vs. n_C for the bands (where $n_C/10$ is effectively the band number or the number of C_{10} molecules in the clusters). The symbol colors identify the number of H_2SO_4 (including the HSO_4^-) in each cluster, as before. Beyond

the first two bands, it is not possible to completely resolve sulfur (mass of 31.97 Da) from two oxygen atoms (total mass of 31.99 Da) when identifying elemental compositions. Moreover, there is always some ambiguity concerning the location of one oxygen atom (O), i.e., whether the anion is HSO_4^- or HSO_5^- (see *SI Text* for details). Consequently, the limiting cases for \overline{OS}_C in bands 3 and 4 are shown with colored bars, assuming either a minimum of one sulfur in all clusters (upper limit for \overline{OS}_C) or a maximum of four sulfur atoms (lower limit for \overline{OS}_C). The circles between the bars show the most probable assignments for individual peaks.

Fig. 2B reveals that the smallest clusters contain organics with a wide range of carbon oxidation states \overline{OS}_C , including extremely highly oxidized organics (e.g., \overline{OS}_C up to 1 for C_{10} compounds), and that both the range of \overline{OS}_C and the average \overline{OS}_C rapidly decrease as the clusters grow. The average \overline{OS}_C converges to an asymptotic value near -0.8 as the clusters grow to contain four organic molecules and up to three sulfur-containing molecules. This result is consistent with the hypothesis that scarce, but highly oxidized organics, which possess many oxygenated functional groups, are effective in initially stabilizing bisulfate anions, whereas subsequent growth is driven by more abundant but less highly oxidized organic species (*SI Text*).

The formulae of the dominant elemental compositions for the PD oxidation products observed in the APi-TOF spectra are not readily associated with products of known oxidation mechanisms (e.g., the master chemical mechanism). Moreover, numerous product molecules participate in the cluster formation and growth, some with a very high degree of oxidation. Because these species are observed to condense on small clusters, they are unambiguously produced in the gas phase, i.e., via gas-phase oxidation starting with PD. The stepwise appearance of growing ion clusters suggests that the participating oxidized organics were typically formed within 5 min from turning on the UV lights. In Fig. 3, we assess PD oxidation using a model based on the 2D volatility basis set (2D-VBS) framework, which describes oxidation of organic compounds classified by volatility ($\log C^o$ on the ordinate, C^o being the compound's saturation concentration) and oxidation state of carbon (\overline{OS}_C on the abscissa) (27, 33–35). Organics are oxidized by OH radicals, forming products distributed in the (C^o , \overline{OS}_C) space. Fig. 3 includes contours for n_O (green) and n_H (cyan), intersecting in a region corresponding roughly to C_{10} molecules. Specific products might appear at the intersection points of these contours, but the exact volatility of these products is not known. Also shown are the location of PD in this space (yellow circle and structure) and contours that

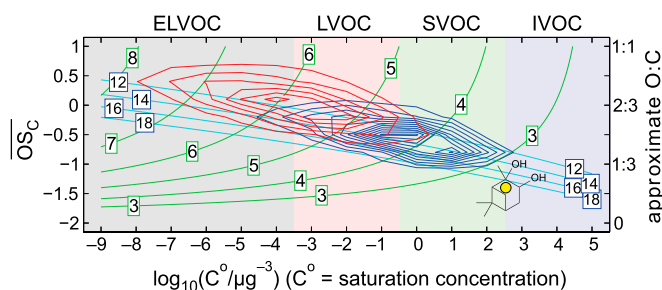


Fig. 3. Representation of PD oxidation in the 2D volatility basis set. Organics are classified as ELVOCs, LVOCs, semivolatile organic compounds (SVOCs), or intermediate volatility organic compounds (IVOCs). PD is shown with a yellow dot. Isolines are exclusively for C_{10} compounds, with oxygen number shown with green curves and hydrogen numbers shown with cyan curves. Blue contours show functionalization products predicted for first-generation PD oxidation using the generic OH oxidation kernel; red contours show functionalization products predicted for second-generation products formed from a distribution of first-generation products weighted by the blue contours.

illustrate how the first- (blue contours) and second- (red contours) generation oxidation products spread from the PD starting location, considering only functionalization, i.e., addition of oxygenated functional groups, while preserving the carbon number (36). The first-generation products are formed directly from PD, whereas the second-generation products form from a distribution of first-generation product classes, weighted by their yields. Although many oxidation products involve smaller fragments ($n_C < 10$), especially in the second generation, our measurements show that C_{10} species dominate the formation of small clusters.

Our experimental observations (Fig. 2B) are quantitatively consistent with the 2D-VBS model. The model predicts that first-generation products of PD oxidation will fall in the range of $-1.25 < \overline{OS}_C < 0$, whereas second-generation products will cover a wider range of oxidation states with $-0.75 < \overline{OS}_C < 0.75$. Generally speaking, organics in the region of the lowest equilibrium vapor pressures [extremely low volatility organic compounds (ELVOCs), with $\log C^\circ < -3.5$] are the most likely to condense on very small molecular clusters, whereas organics in the lower half of the LVOC region ($-3.5 < \log C^\circ < -0.5$) should be able to drive growth of clusters beyond a certain size (22). We thus expect, and indeed observe, that highly oxidized second-generation PD products (ELVOCs) most effectively form stable complexes with single H_2SO_4 molecules (evident in the high \overline{OS}_C for C_{10} clusters; Fig. 2B) and that somewhat less oxidized, but more abundant, first-generation products drive the initial growth of the clusters (evident in the declining average \overline{OS}_C as the clusters grow). However, it is striking that a fairly broad range of organic species can participate in cluster formation and growth (evident in the ranges of \overline{OS}_C observed throughout; Fig. 2B).

Ion Clusters in Comparison with Neutral Clusters. The primary subject of this study is our experiments in the system of H_2SO_4 and oxidized organics. The observed formation rate of 1.7-nm particles was about $10 \text{ cm}^{-3} \cdot \text{s}^{-1}$ at $[H_2SO_4] = 10^7 \text{ cm}^{-3}$, consistent

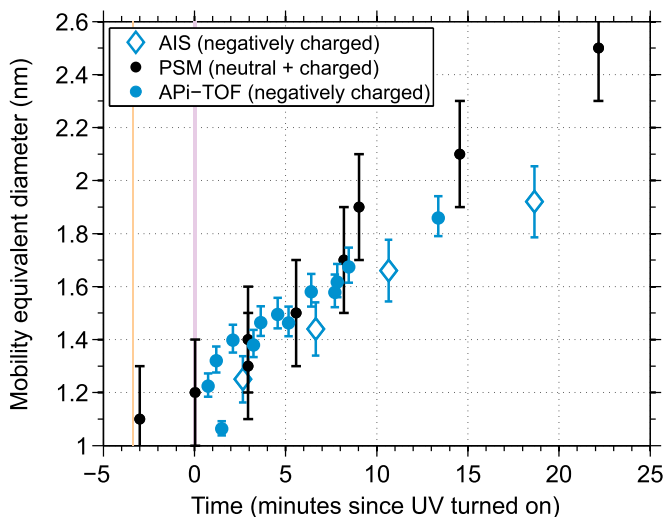


Fig. 4. Appearance times of neutral plus charged clusters from the PSM (black circles) and of negatively charged clusters from the API-TOF (blue circles) and an air ion spectrometer that measures ion mobility directly (AIS, blue diamonds), for the beginning of an example new particle formation experiment, initiated by UV illumination. Vertical error bars correspond to deviations in assumed densities by $\pm 200 \text{ kg} \cdot \text{m}^{-3}$ (API-TOF), the range of cutoff diameters in instrument calibrations (PSM, $\pm 0.2 \text{ nm}$), or the widths of size channels (AIS, $\pm 7\%$). The vertical bars show when the high-voltage clearing field in the CLOUD chamber was turned off (red) and when the UV lights in the CLOUD chamber were turned on (purple).

with ambient observations. Under those conditions, the formation rate was only weakly dependent on charge. Also, neutral new particle formation and growth generally dominates in ambient observations within the planetary boundary layer (3, 37). All experimental data shown here are from negatively charged clusters. However, the composition of the negatively charged clusters is likely similar to the composition of the neutral clusters, particularly for clusters containing oxidized organics and H_2SO_4 .

The first indication of such similarity is the experimental observation in the CLOUD chamber, which show comparable growth rates in the 1- to 2-nm size range observed by both the API-TOF and condensation particle counters. Condensation particle counters, such as the particle size magnifier (PSM) (38), detect both charged and neutral clusters, but agreement with the API-TOF includes events dominated by neutral formation and growth. A PSM with a variable cutoff size was used here to obtain size-resolved number concentrations in the size range of 1–2.5 nm in mobility-equivalent diameter (3, 39). To compare their temporal evolution to that of the ion mass spectra, we translate the ion masses to mobility-equivalent diameters and determine the appearance times of the ions (*SI Text*). The appearance times of all particles and those of negatively charged particles typically agree within the uncertainties of the method (Fig. 4). This agreement suggests that the formation and growth mechanisms of ion clusters are indeed similar to those of neutral clusters. In these conditions, the observations do not show an enhancement of growth rate of charged clusters compared with the growth rate of neutral clusters, contrary to suggestions in other studies (40, 41).

The second indication results from quantum chemical calculations. These yield similar structures for neutral and anionic clusters with the same constituents. In particular in the case of clusters containing oxidized organic compounds, the oxidized organic compounds will most likely be acids. Thus, when charging such a cluster by removal of a proton, the organic acid will probably stay in the cluster and the composition of the cluster will be maintained. However, clusters containing the bases ammonia or DMA will lose some ammonia or DMA when they obtain a negative charge, due to the generation of an unbalanced bisulfate ion, which itself is a Lewis base (an electron donor) and competes with ammonia or DMA (42). Therefore, the number of ammonia and DMA molecules in negatively charged clusters is a lower bound for the number in the corresponding neutral cluster.

Conclusions

Of all of the chemical mixes investigated in the CLOUD chamber, the system of H_2SO_4 and oxidized organics described here comes closest to matching ambient new particle formation events in a boreal forest, providing strong evidence that such oxidized organics very likely play a critical role in formation events in the planetary boundary layer.

The API-TOF spectra provide important constraints on clustering interactions between H_2SO_4 and oxidized organics. We showed that large oxidized organics, some of them highly oxidized, are produced rapidly from the gas phase oxidation of pinanediol (a model for first-generation products of monoterpenes) and that, together with H_2SO_4 , they participate in the initial formation and growth of ion clusters from the very first step onward. The 2D-VBS model demonstrates that they can be formed by oxidation of less oxidized precursors; however, the detailed mechanism driving this extensive oxidation remains unknown. It is likely that electrically neutral clusters form and grow via very similar mechanisms. Our observations are direct experimental proof of the hypothesis that later-generation products from the gas phase oxidation of volatile organic compounds, particularly of monoterpenes, contribute to the formation and growth of atmospheric aerosol.

State-of-the-art experimental techniques allow us to develop the chemical fingerprints of a gallery of processes suspected of playing

a role in atmospheric new particle formation. By combining measurements of the chemistry of new particle formation events (composition of growing clusters), as shown here, and the physics of the same events (formation and growth rates), we thus developed the means for far more specific diagnostics of this important process, and we moved a decisive step closer to revealing the exact mechanisms by which new particle formation proceeds in the atmosphere.

Methods

The CLOUD facility at CERN is one of the most advanced laboratory environments for the study of the formation and initial growth of particles (9). It provides exceptionally clean and well-defined experimental conditions in a cylindrical 26.1-m³ stainless steel reaction chamber. Very low concentrations of H₂SO₄, bases such as ammonia and amines, and organics can be controlled and measured. The chamber is filled with ultrapure N₂, O₂, H₂O, and O₃ and is precisely (± 0.01 K) temperature controlled between -65 and $+100$ °C. A pion beam can be provided by the CERN Proton Synchrotron to increase the ion production rate in the CLOUD chamber, and a high-voltage clearing field can be turned on to rapidly remove any ions to ensure electrically neutral conditions.

For all experiments at the CLOUD chamber discussed here, the temperature was 5 °C and the relative humidity was 40%, unless otherwise noted. SO₂ was typically added as a precursor for H₂SO₄, whereas NH₃, DMA, and other organics were added as needed. OH radicals were formed via UV photolysis of O₃ to oxidize both SO₂ to form H₂SO₄ and organics that form condensable organic vapors. Fresh gas was continuously fed into the CLOUD

chamber at a rate of around 100 L/min, and an array of instruments sampled air at the same total rate from the chamber through ports arranged radially around the chamber. The main subject of this study is data obtained from the API-TOF (Tofwerk AG and Aerodyne Research) mass spectrometer as described in detail by Junninen et al. (26). The data were analyzed using the latest versions of tofTools, a MATLAB-based software package in development by the University of Helsinki.

See *SI Text* for a more detailed description of the experimental setup and methods.

ACKNOWLEDGMENTS. The European Organization for Nuclear Research (CERN)'s support of CLOUD with important technical and financial resources and provision of a particle beam from the Proton Synchrotron is gratefully acknowledged. This research was funded by the European Commission 7th Framework Programme (Marie Curie Initial Training Network "CLOUD-ITN," Grant 215072), the European Research Council (ERC) Advanced Grant Atmospheric nucleation: from molecular to global scale (ATMNUCLE) (Grant 227463), the ERC Starting Grant "Role of Molecular Clusters in Atmospheric Particle Formation (MOCAPAF)" (Grant 257360), the Academy of Finland via the Centre of Excellence Programme (Project 1118615) and Grant 1133872, the German Federal Ministry of Education and Research (Project 01LK0902A), the Swiss National Science Foundation (Projects 206621_125025 and 206620_130527), the Austrian Science Fund (Projects P19546 and L593), the Portuguese Foundation for Science and Technology (Project CERN/FP/116387/2010), the Russian Foundation for Basic Research (Grant N08-02-91006-CERN), the Davidow Foundation, the Royal Society Wolfson Research Award, and the US National Science Foundation (Grants AGS1136479 and CHE1012293).

- Makkonen R, et al. (2012) Air pollution control and decreasing new particle formation lead to strong climate warming. *Atmos Chem Phys* 12(3):1515–1524.
- Vehkamäki H, Riipinen I (2012) Thermodynamics and kinetics of atmospheric aerosol particle formation and growth. *Chem Soc Rev* 41(15):5160–5173.
- Kulmala M, et al. (2013) Direct observations of atmospheric aerosol nucleation. *Science* 339(6122):943–946.
- Riipinen I, et al. (2012) The contribution of organics to atmospheric nanoparticle growth. *Nat Geosci* 5(7):453–458.
- Weber RJ, et al. (1996) Measured atmospheric new particle formation rates: Implications for nucleation mechanisms. *Chem Eng Commun* 151(1):53–64.
- Sihto S-L, et al. (2006) Atmospheric sulphuric acid and aerosol formation: Implications from atmospheric measurements for nucleation and early growth mechanisms. *Atmos Chem Phys* 6(12):4079–4091.
- Kuang C, McMurry PH, McCormick AV, Eisele FL (2008) Dependence of nucleation rates on sulfuric acid vapor concentration in diverse atmospheric locations. *J Geophys Res Atmos* 113(D10):D10209.
- Sipilä M, et al. (2010) The role of sulfuric acid in atmospheric nucleation. *Science* 327(5970):1243–1246.
- Kirkby J, et al. (2011) Role of sulphuric acid, ammonia and galactic cosmic rays in atmospheric aerosol nucleation. *Nature* 476(7361):429–433.
- Ortega IK, Kurtén T, Vehkamäki H, Kulmala M (2008) The role of ammonia in sulfuric acid ion induced nucleation. *Atmos Chem Phys* 8(11):2859–2867.
- Kurtén T, Loukonen V, Vehkamäki H, Kulmala M (2008) Amines are likely to enhance neutral and ion-induced sulfuric acid-water nucleation in the atmosphere more effectively than ammonia. *Atmos Chem Phys* 8(14):4095–4103.
- Paasonen P, et al. (2012) On the formation of sulphuric acid – amine clusters in varying atmospheric conditions and its influence on atmospheric new particle formation. *Atmos Chem Phys* 12(19):9113–9133.
- Zhang R, et al. (2004) Atmospheric new particle formation enhanced by organic acids. *Science* 304(5676):1487–1490.
- Zhao J, Khalizov A, Zhang R, McGraw R (2009) Hydrogen-bonding interaction in molecular complexes and clusters of aerosol nucleation precursors. *J Phys Chem A* 113(4):680–689.
- Metzger A, et al. (2010) Evidence for the role of organics in aerosol particle formation under atmospheric conditions. *Proc Natl Acad Sci USA* 107(15):6646–6651.
- Hou G-L, et al. (2013) Negative ion photoelectron spectroscopy reveals thermodynamic advantage of organic acids in facilitating formation of bisulfate ion clusters: Atmospheric implications. *J Phys Chem Lett* 4(5):779–785.
- Nadykto AB, Yu F, Jakovleva MV, Herb J, Xu Y (2011) Amines in the earth's atmosphere: A density functional theory study of the thermochemistry of pre-nucleation clusters. *Entropy* 13(2):554–569.
- Paasonen P, et al. (2010) On the roles of sulphuric acid and low-volatility organic vapours in the initial steps of atmospheric new particle formation. *Atmos Chem Phys* 10(22):11223–11242.
- Ortega IK, et al. (2012) New insights into nocturnal nucleation. *Atmos Chem Phys* 12(9):4297–4312.
- Zhang R, et al. (2009) Formation of nanoparticles of blue haze enhanced by anthropogenic pollution. *Proc Natl Acad Sci USA* 106(42):17650–17654.
- Wang L, et al. (2010) Atmospheric nanoparticles formed from heterogeneous reactions of organics. *Nat Geosci* 3(4):238–242.
- Donahue NM, Trump ER, Pierce JR, Riipinen I (2011) Theoretical constraints on pure vapor-pressure driven condensation of organics to ultrafine particles. *Geophys Res Lett* 38(16):L16801.
- Kuang C, et al. (2012) Size and time-resolved growth rate measurements of 1 to 5nm freshly formed atmospheric nuclei. *Atmos Chem Phys* 12(7):3573–3589.
- Riipinen I, et al. (2011) Organic condensation: A vital link connecting aerosol formation to cloud condensation nuclei (CCN) concentrations. *Atmos Chem Phys* 11(8):3865–3878.
- Riccobono F, et al. (2012) Contribution of sulfuric acid and oxidized organic compounds to particle formation and growth. *Atmos Chem Phys* 12(20):9427–9439.
- Junninen H, et al. (2010) A high-resolution mass spectrometer to measure atmospheric ion composition. *Atmos Meas Tech* 3(4):1039–1053.
- Donahue NM, et al. (2012) Aging of biogenic secondary organic aerosol via gas-phase OH radical reactions. *Proc Natl Acad Sci USA* 109(34):13503–13508.
- Ehn M, et al. (2012) Gas phase formation of extremely oxidized pinene reaction products in chamber and ambient air. *Atmos Chem Phys* 12(11):5113–5127.
- Almeida J, et al. (2013) Molecular understanding of amine-sulphuric acid particle nucleation in the atmosphere. *Nature*, 10.1038/nature12663.
- Vana M, et al. (2006) Charging state of atmospheric nanoparticles during the nucleation burst events. *Atmos Res* 82(3–4):536–546.
- Kerminen V-M, et al. (2010) Atmospheric nucleation: Highlights of the EUCAARI project and future directions. *Atmos Chem Phys* 10(22):10829–10848.
- Kroll JH, et al. (2011) Carbon oxidation state as a metric for describing the chemistry of atmospheric organic aerosol. *Nat Chem* 3(2):133–139.
- Donahue NM, Epstein SA, Pandis SN, Robinson AL (2011) A two-dimensional volatility basis set: 1. organic-aerosol mixing thermodynamics. *Atmos Chem Phys* 11(7):3303–3318.
- Donahue NM, Kroll JH, Pandis SN, Robinson AL (2012) A two-dimensional volatility basis set – Part 2: Diagnostics of organic-aerosol evolution. *Atmos Chem Phys* 12(2):615–634.
- Murphy BN, et al. (2012) Functionalization and fragmentation during ambient organic aerosol aging: Application of the 2-D volatility basis set to field studies. *Atmos Chem Phys* 12(22):10797–10816.
- Kroll JH, et al. (2009) Measurement of fragmentation and functionalization pathways in the heterogeneous oxidation of oxidized organic aerosol. *Phys Chem Chem Phys* 11(36):8005–8014.
- Manninen HE, et al. (2010) EUCAARI ion spectrometer measurements at 12 European sites - Analysis of new particle formation events. *Atmos Chem Phys* 10(16):7907–7927.
- Vanhanen J, et al. (2011) Particle size magnifier for nano-CN detection. *Aerosol Sci Technol* 45(4):533–542.
- Kulmala M, et al. (2012) Measurement of the nucleation of atmospheric aerosol particles. *Nat Protoc* 7(9):1651–1667.
- Nadykto AB, Yu F (2003) Uptake of neutral polar vapor molecules by charged clusters/particles: Enhancement due to dipole-charge interaction. *J Geophys Res-Atmos* 108:(D23):4717.
- Lushnikov A, Kulmala M (2004) Charging of aerosol particles in the near free-molecule regime. *Eur Phys J D* 29(3):345–355.
- Kurtén T, et al. (2011) The effect of H₂SO₄-amine clustering on chemical ionization mass spectrometry (CIMS) measurements of gas-phase sulfuric acid. *Atmos Chem Phys* 11(6):3007–3019.